Supplementary Information

Measurement of the Interconnected Turgor Pressure and Envelope Elasticity of Live Bacterial Cells

Huanxin Zhang,[a] Huabin Wang,[*bcd] Jonathan J. Wilksch,[e] Richard A. Strugnell,[f] Michelle L. Gee,[g] and Xi-Qiao Feng[*a]

1. LIVE/DEAD Fluorescence Cell Assays

Cell viability was assessed with a LIVE/DEAD BacLight Bacterial Viability Kit (Molecular Probes) containing SYTO9 and propidium acid nucleic acid stains. Capsule-deficient *K. pneumoniae* cells were adhered to gelatin-coated glass disks prepared by the same method as for the AFM experiments. The disks were submerged in either Milli-Q water or 100 mM $CaCl_2$ solution for different time points, and then treated with a mixture of the stains. Viable and dead bacterial cells were fluorescently stained green or red, respectively. Cells were visualized, and images were captured using an inverted fluorescence microscope (DM14000B; Leica). For each type of cell, three independent samples in either Milli-Q water or 100 mM $CaCl_2$ solution were analyzed at each time point. Cells were counted using the 'Analyze Particles' function in ImageJ.

The ratio of damaged cells (red) to intact cells (green) was below 5% for up to 6 hours in the two different osmotic conditions (Fig. S1), indicating that the vast majority of cells remained viable in either Milli-Q water or 100 mM $CaCl_2$ solution during the AFM experiments. The adaptation to osmotic stress is an intrinsic ability of bacteria,[1] and they utilize different mechanisms to survive in various liquid environments with substantially varying osmolality.[2]

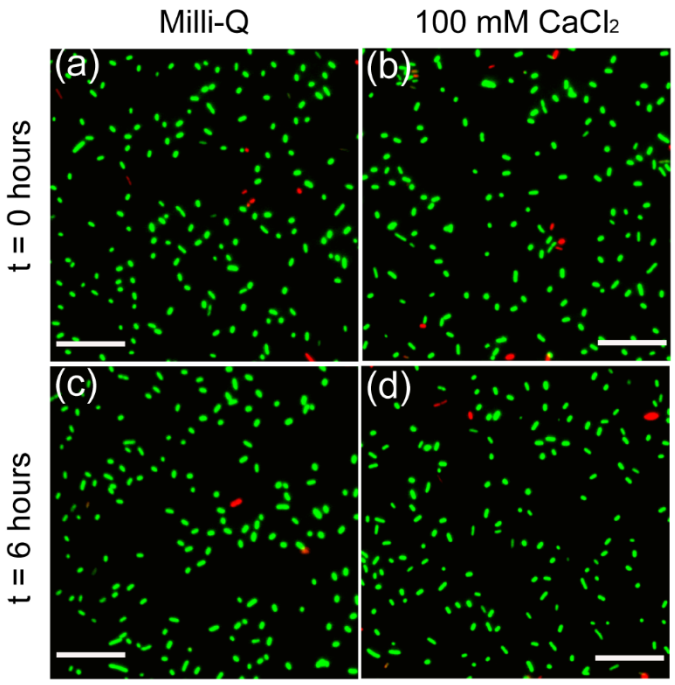

Fig. S1 Fluorescence images of capsule-deficient *K. pneumoniae* after immersion in different osmotic conditions. (a and c) are images of cells submerged in Milli-Q for 0 h (control) and 6 h (experimental group), respectively. (b and d) are images of cells submerged in 100 mM $CaCl_2$ solution for 0 h (control) and 6 h (experimental group), respectively. Scale bars: 20 μm.

2. Governing Relations Involved in the Indentation of a Bacterial Cell

The cell envelope can be regarded as a stress-stiffening and orthotropic elastic material.[3-5] Since the cell envelope thickness is much less than the cellular radius ($t/R < 0.1$), thin shell approximation can be adopted.[6] Therefore, the stress in the thickness direction is negligible, and only the in-plane stresses in the axial and circumferential directions need to be considered. The constitutive relationships between the incremental strain tensors ($\mathrm{d}\varepsilon_z$, $\mathrm{d}\varepsilon_\theta$, and $\mathrm{d}\varepsilon_{\theta z}$) and the incremental stress tensors ($\mathrm{d}\sigma_\theta$, and $\mathrm{d}\tau_{\theta z}$) can be given by[7]

$$\mathrm{d}\varepsilon_z = \frac{\mathrm{d}\sigma_z}{E_{\parallel}}, \mathrm{d}\varepsilon_\theta = \frac{\mathrm{d}\sigma_\theta}{E_{\perp}}, \mathrm{d}\varepsilon_{\theta z} = \frac{\mathrm{d}\tau_{\theta z}}{G} \tag{S.1}$$

where z and θ are the cylindrical coordinates; G, $E_{\perp}$ and $E_{\parallel}$ are the shear modulus, and the Young's moduli in the circumferential and axial directions, respectively. According to previous work,[3] the cell envelope can be stiffened by turgor pressure, and the relationship between the circumferential Young's modulus ($E_{\perp}$) and the turgor pressure (p) can be expressed as $E_{\perp} = E_0 \left(p / p_0 \right)^{\gamma}$, where E_0 is the elastic modulus at a reference turgor pressure, p_0, and the stress-stiffening factor, γ, is 1.22.

The strain-displacement relations for the bacterial cell can be given by

$$\varepsilon_z = \frac{\partial u_z}{\partial z}, \varepsilon_\theta = \frac{1}{R}\frac{\partial u_\theta}{\partial \theta} - \frac{u_r}{R}, \varepsilon_{\theta z} = \frac{1}{R}\frac{\partial u_z}{\partial \theta} + \frac{\partial u_\theta}{\partial z} \tag{S.2}$$

where u_z, u_θ and u_r are the displacement components in the axial, circumferential and radial directions, respectively.

During AFM indentation, the bacterial cell balances the force exerted by the AFM probe. Because the bacterial cell was fixed on a substrate during the indentation, the inertial motion was negligible. In the absence of body forces, the stress tensors satisfy the equilibrium equation, $\mathrm{div}\,\boldsymbol{\sigma} = 0$. For a thin cylindrical shell with a radius of R, we have the following equations in the axial and circumferential directions:

$$\frac{1}{R}\frac{\partial \sigma_\theta}{\partial \theta} + \frac{\partial \tau_{\theta z}}{\partial z} = 0, \frac{1}{R}\frac{\partial \tau_{\theta z}}{\partial \theta} + \frac{\partial \sigma_z}{\partial z} = 0 \tag{S.3}$$

In addition, the turgor pressure p is balanced by the equivalent elasticity of the cell envelope. The boundary condition of the inner surface of the cell envelope can be expressed as

$$\sigma_\theta t = -pR \tag{S.4}$$

where $\sigma_\theta t$ is the circumferential surface tension.

The displacement boundary condition of the outer surface ($r = R, \theta = \pi/2, z = 0$) of the cell envelope can be expressed by

$$u_r\left(R, \pi/2, 0\right) = -\delta \tag{S.5}$$

where δ represents the indentation depth.

Based on eqn (S.1) – (S.5), FEM simulations were performed to investigate the AFM-based nanoindentation of individual bacterial cells, and the scaling rules were derived to determine the turgor pressure and the Young's modulus of the cell envelope.

3. The Bacterial 'Indentation rule' and 'Expansion rule'

Dimensional analysis is a widely used method to establish the scaling rules for dimensionless physical and geometrical parameters involved in experiments.[8-10] The scaling rules obtained from dimensional analysis provided guidelines for the FEM simulations of indentation. The combination of dimensional analysis and FEM simulations enabled us to establish the scaling rules to quantify the nanoindentation response of bacterial cells.

For the cell envelope of a bacterium, the nanoindentation force is a function of seven independent parameters:

$$F = f\left(\delta; E_\perp, E_{||}, p, R, t, \rho\right) \tag{S.6}$$

where ρ is the curvature radius of the AFM probe.

In our simulation, the bacterial cell was modeled as a tube shape terminated with two semi-spherical caps. Radial expansion of the cylindrical envelope under turgor pressure is governed by

the elasticity of the cylinder in the circumferential direction, $E_{\perp}$.[3] The bacterial radius (R) under turgor pressure is a function of the reference radius R_0, $E_{\perp}$, p and t, which is expressed as

$$R = g\left(E_{\perp}, p, t, R_0\right) \tag{S.7}$$

where R_0 is the radius of the bacterium at a reference pressure p_0. The introduction of p_0 and R_0 is just required for obtaining dimensionless relationships (scaling rules) of the physical parameters involved in the radial expansion of inflated cylinder. The two parameters have little effect on the scaling rules, and the extracted turgor pressure and Young's modulus from the experimental data. In this study, we selected a physiological turgor pressure (29 kPa) of Gram-negative rod-shape bacteria as the reference turgor pressure.[3]

For thin shells ($t/R < 0.1$), we derived the following scaling rules according to the Kirchhoff–Love theory:[6]

$$f\left(\delta; \alpha E_{\perp}, E_{\parallel}, p, R, \alpha^{-1}t, \rho\right) = f\left(\delta; E_{\perp}, E_{\parallel}, p, R, t, \rho\right) \tag{S.8}$$

$$g\left(\alpha E_{\perp}, p, \alpha^{-1}t, R_0\right) = g\left(E_{\perp}, p, t, R_0\right) \tag{S.9}$$

where α is a scale factor.

We can further obtain the following equations:[3]

$$f\left(\delta; \beta E_{\perp}, \beta E_{\parallel}, \beta p, R, t, \rho\right) = \beta f\left(\delta; E_{\perp}, E_{\parallel}, p, R, t, \rho\right) \tag{S.10}$$

$$g\left(\beta E_{\perp}, \beta p, t, R_0\right) = g\left(E_{\perp}, p, t, R_0\right) \tag{S.11}$$

$$f\left(\eta\delta; E_{\perp}, E_{\parallel}, p, \eta R, \eta t, \eta\rho\right) = \eta^2 f\left(\delta; E_{\perp}, E_{\parallel}, p, R, t, \rho\right) \tag{S.12}$$

$$g\left(E_{\perp}, p, \eta t, \eta R_0\right) = \eta g\left(E_{\perp}, p, t, R_0\right) \tag{S.13}$$

where η and β are scale factors.

By combining eqn (S.6), (S.8), (S.10) and (S.12), while taking the circumferential Young's modulus $E_\perp$ and the cell envelope thickness t as basic quantities and applying the Buckingham Π theorem,[11] eqn (S.6) was formulated as

$$F = E_\perp t^2 \Pi\left(\frac{\delta}{t}; \frac{pR}{E_\perp t}, \frac{E_\parallel}{E_\perp}, \frac{\rho}{t}\right) \tag{S.14}$$

where Π is a dimensionless function, and $E_\parallel / E_\perp$ is the orthotropic elastic ratio and termed 'α'. α is a function of surface tension and given by:[3]

$$\alpha = \frac{1}{2^\gamma} \frac{1 - \left[\bar{p}\gamma\left(\bar{\sigma}^{1-\gamma}/2^{1-\gamma} - 1\right)/(1-\gamma)\right]}{1 - \left[\bar{p}\gamma\left(\bar{\sigma}^{1-\gamma} - 1\right)/(1-\gamma)\right]} \tag{S.15}$$

where the dimensionless parameters are defined as $\bar{p} = p_0 R_0 / (E_0 t)$, and $\bar{\sigma} = pR/(p_0 R_0)$.

AFM nanoindentation experiments show that the force F depends linearly on the indentation depth δ for the measured deformation region, indicating that the cell stiffness is independent on δ in this region. By further taking into account that *t* is a constant, the scaling rule for the cell stiffness can be derived from eqn (S.14) and expressed as:

$$k = \frac{dF}{d\delta} = E_\perp t \Pi'\left(\frac{pR}{E_\perp t}, \alpha, \frac{\rho}{t}\right) \tag{S.16}$$

where $E_\perp t$ represents the lateral stretching modulus in the shell theory.[5] From eqn (S.16), it can be seen that $k/(E_\perp t)$ only depends on $pR/(E_\perp t)$, the orthotropic elastic ratio α and the scaled probe radius ρ/t.

According to the AFM probe manufacture's specifications, the nominal curvature radius and cone angle of the probe are 20 nm and 15°, respectively. In the FEM simulation, we have tested probes with tip curvature radii between 6 to 25 nm ($\rho/t = 0.2 \sim 0.9$) at varied cone angles from

10 to 30°, and found that the dimensionless stiffness. $k/(E_\perp t)$. was independent on the curvature radius of the AFM probe (Fig. S2a). On the other hand, we also found that the value of α was ~ 0.47 (Fig. S2b) by using eqn (S. 15) for a wide range of scaled tension $\bar{\sigma}$ (set the turgor pressure p from 1 to 500 kPa and the turgor-free radius from 300 to 600 nm), and implying that the effect of the orthotropic elastic ratio on $k/(E_\perp t)$ in the investigated region is negligible. As a result, from eqn (S16), the bacterial 'indentation rule' can be obtained:

$$k = E_\perp t \Pi_1\left(\frac{pR}{E_\perp t}\right) \tag{S.17}$$

where $\Pi_1 = \Pi'$.

Similarly, by applying the Buckingham Π theorem and scaling rules (eqn (S.9), (S.11) and (S.13)) to eqn (S.7), we can obtain the bacterial 'Expansion rule', expressed as:

$$\frac{R}{R_0} = \Pi_2\left(\frac{E_\perp t}{pR_0}\right) \tag{S.18}$$

where Π_2 is a dimensionless function. According to eqn (S.18), the dependence of R/R_0 on $E_\perp t/(pR_0)$ can be explicitly solved.

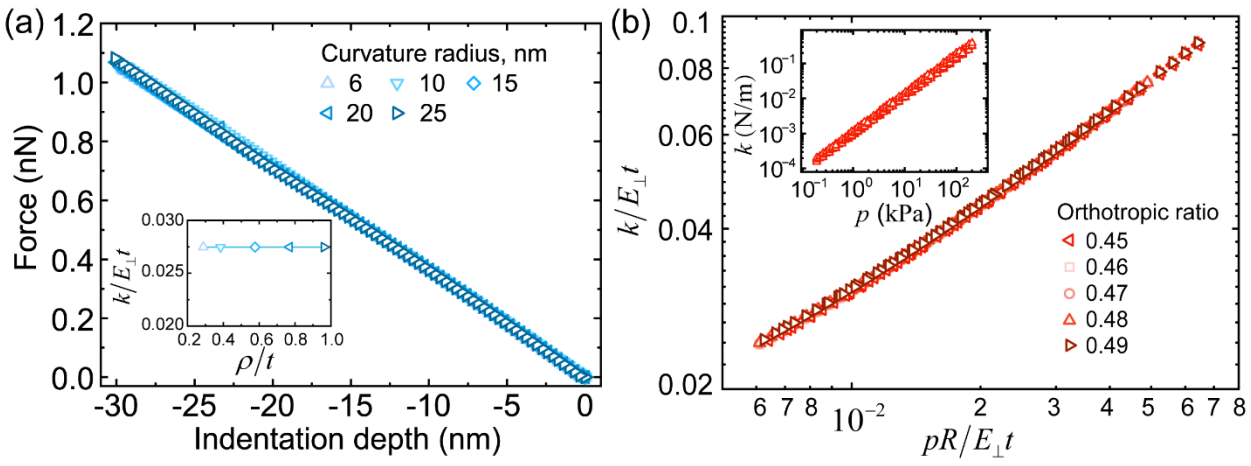

Fig. S2 Effects of the curvature radius of the AFM tip and the orthotropic elastic ratio on indentation response. (a) Indentation curves under different probe radii. *Inset* shows the reduced stiffness $k/E_{\perp}t$ under the scaled probe radius ρ/t. (b) The reduced stiffness vs. $pR/E_{\perp}t$ for different ratios α, namely, 0.45, 0.46, 0.47, 0.48 and 0.49. Inset shows the indentation stiffness. k. against the turgor pressure p in log-log plot.

According to the scaling rules shown in eqn (S.17) and (S.18), the dimensionless stiffness and radius are only determined by the dimensionless parameters $pR/(E_{\perp}t)$ and $E_{\perp}t/(pR_0)$, respective. We selected a physiological turgor pressure (29 kPa) of Gram-negative rod-shape bacteria as the reference turgor pressure and simulated the nanoindentation of individual cells with turgor pressure within the range of 1 – 500 kPa.[3, 5, 12] In the simulations, the reference Young's modulus of the cell envelope E_0, the stress-stiffening exponent γ, the orthotropic ratio α, equivalent envelope thickness t, turgor-free bacterial radius R_f, and the cell cylindrical part length L_{cy} were set at 49 MPa, 1.22, 0.47, 26 nm, 500 nm, and 2000 nm, respectively.[3] By fitting the FEM simulated data (Fig. 4), we obtained closed forms of the scaling rules, expressed as:

$$\frac{k}{E_{\perp}t} = \Pi_1\left(\frac{pR}{E_{\perp}t}\right) = a\ln\left(\frac{pR}{E_{\perp}t} + b\right) + c \tag{S.19}$$

$$\frac{R}{R_0} = \Pi_2\left(\frac{E_{\perp}t}{pR_0}\right) = \frac{E_{\perp}t/pR_0 - A}{B\cdot E_{\perp}t/pR_0 + C} \tag{S.20}$$

where the coefficients $a = 0.09$, $b = 0.05$, $c = 0.28$, $A = 0.18$, $B = 0.95$, $C = 4.47$.

These fitting coefficients depict important features of the expansion rule (Fig. S3). Constant A, $A = E_0 t/(p_0 R_0)\cdot(p_{\min}/p_0)^{\gamma-1}$, denotes the minimum of the dimensionless quantity for the case of the scaled radius close to zero, corresponding to the possible minimum of turgor pressure ($p_{\min}$) for the collapse state of bacterial cells. Constant B, $B = R_0/R_{\max}$, is associated with the maximum scaled cell radius, which means that bacteria can prevent abrupt cell shape change during changes in external osmotic environment. This is consistent with the stress-stiffening effect of the bacterial cell. In addition, constant C describes the expansion rate as the dimensionless quantity $E_\perp t/pR_0$.

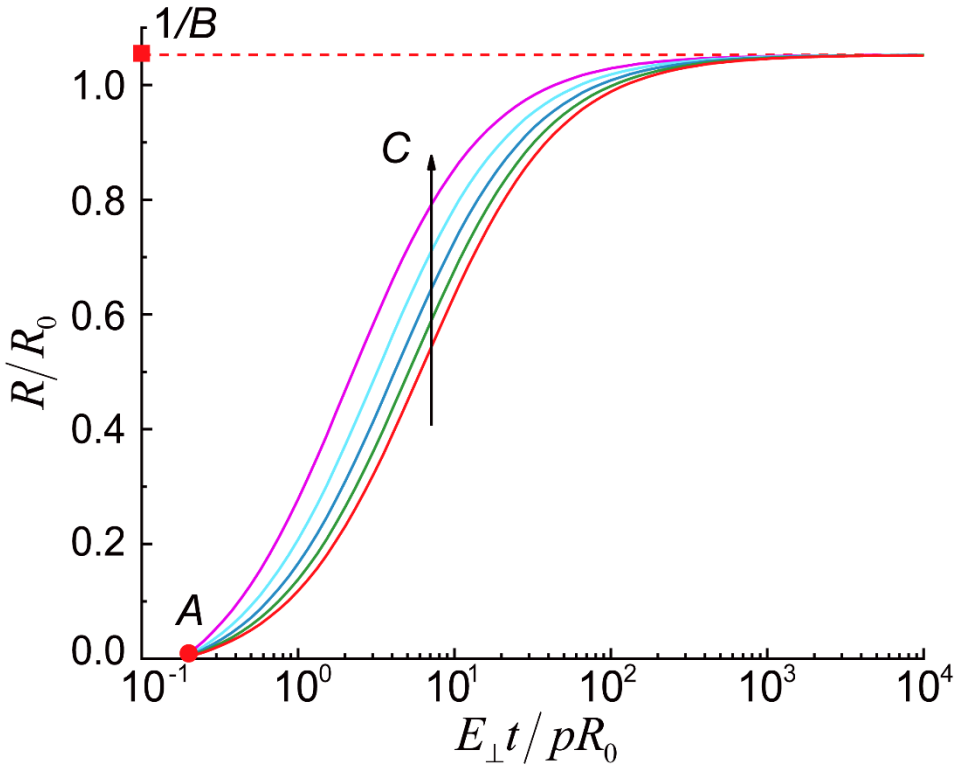

Fig. S3 The meaning of the fitting coefficients A, B, and C in the expansion rule. A (circle point) represents the value of $E_\perp t/pR_0$ for the case of the scaled radius close to zero. $1/B$ is the maximum scaled cell radius (square point). C controls the expansion rate of the bacterial cell as the dimensionless quantity $E_\perp t/pR_0$ increases. In this example, the values of the parameters are:

A, 0.18; *B*, 0.95; *C*, {2, 3, 4, 5, 6}.

4. Applicability of the Developed Scaling Rules to Bacterial Cells with Different Physical Parameters

Due to the individualisms of bacteria, bacterial cells can be different in lengths, radii and envelope thicknesses. Therefore, it is necessary to examine whether our developed rules can be applied to cells with varied physical parameters or not. Firstly, we investigated the influence of the bacterial length on the cell stiffness. A representative example is shown in Fig. S4a, from which we can see that the cell stiffness is nearly a constant (0.041 ± 0.001 N/m) and independent on the cell length (0.5 to 3.0 μm for the turgor-free length of the cylindrical part of the cell). This can be easily understood by considering that the length scale of the contact between the AFM tip and the bacterial envelope in our system is in the order of 10 nm, which is about two orders of magnitude smaller than the length scale (μm) of the cylindrical part of the cell. Then, we verified the applicability of the 'Indentation rule' (eqn (S.19)) to bacterial cells with different turgor-free radii (R_f, 300 – 600 nm) and envelope thicknesses (20 – 45 nm) under turgor pressures from 1 to 500 kPa. Representative results are shown in Fig. S4b and c, respectively, from which it can be observed that the 'Indentation rule' is in well agreement with the FEM simulated data. Finally, we tested the applicability of the 'Expansion rule' (eqn (S.20)) to bacterial cells with different turgor-free radii (300 – 600 nm) and envelope thicknesses (20 – 45 nm) under turgor pressures from 1 to 500 kPa. Representative examples are demonstrated in Fig. S4d and e, respectively, from which it can be seen that the 'Expansion rule' is highly consistent with the FEM simulated data. According to the available information, here we have considered all of the possible lengths, radii, envelope thicknesses and turgor pressure of rod-shape Gram-negative bacteria that could be measured in real experiments. The above results confirm that our scaling rules (eqn (S.19) and (S.20)) can be

well applied to extract the turgor pressure and envelope elasticity of rod-shape Gram-negative bacteria.

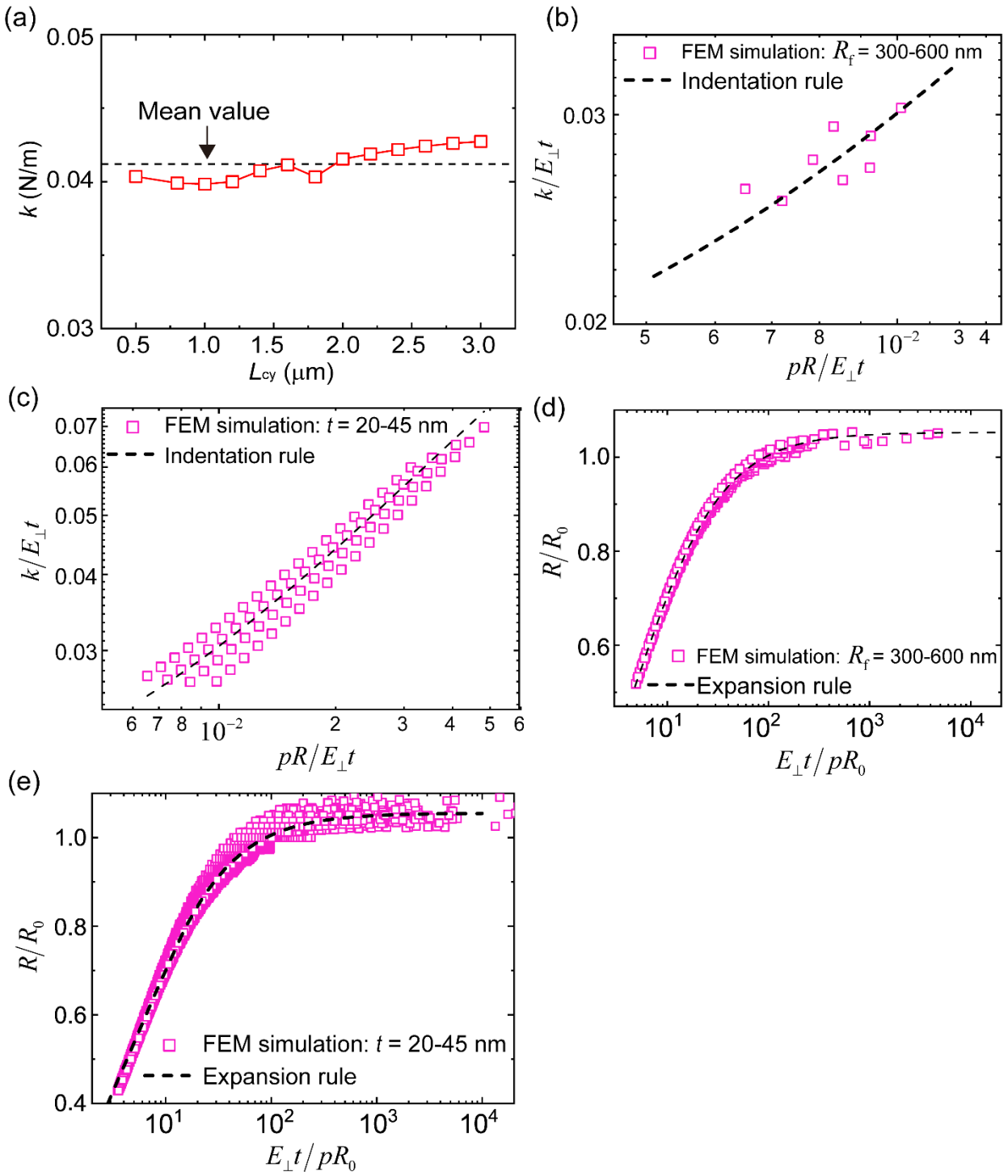

Fig. S4 Verification of the applicability of the scaling rules to rod-shape bacteria with various lengths (of the cylindrical part of the cell), radii and envelope thicknesses under a wide range of turgor pressure. (a) FEM simulated stiffness (red square) of bacterial cell with different lengths (0.5 to 3.0 μm for the turgor-free length of the cylindrical part of the cell). The dashed line indicates the mean value (0.041 N/m) of the simulated data. In the FEM simuations, the turgor-free radius of the cell, cell envelope thickness, and reference turgor pressure were set at 500 nm, 26 nm, and 29 kPa, respectively. The scaling rules are compared with the FEM simulation results for cells (b and d) with different turgor-free radii (300 – 600 nm), and (c, e) with different envelope thicknesses (20 – 45 nm) under turgor pressures from 1 to 500 kPa. Other parameters used in the FEM simulations for (a-e) include : ρ = 20 nm; $E_0 = 49$ MPa ; $\gamma = 1.22$; $\alpha = 0.47$.

5. Fitting the Experimental Data with the Bacterial 'Indentation Rule' and the 'Expansion Rule'

5.1 Procedures of Using the Rules to Extract Turgor Pressure and Envelope Elasticity

The experimental data can be fitted by using our developed rules to obtain the cell envelope elasticity and cell turgor pressure. Firstly, the cell stiffness (k) and radius (R) were measured from the AFM nanoindentation force profile and AFM topographical image of the cell. Secondly, when $p = p_0$, we have $R = R_0$, then $E_0 t/(p_0 R_0)$ can be derived from eqn (S.20), viz:

$$\frac{E_0 t}{p_0 R_0} = \frac{A + C}{1 - B} = \xi \tag{S.21}$$

Thirdly, we can rewrite the scaled inflated radius R/R_0 as eqn (S.22) by substituting ξ and $E_\perp = E_0 (p/p_0)^\gamma$ into eqn (S.20):

$$\frac{R}{R_0}=\left(\xi\left(\frac{p}{p_0}\right)^{\gamma-1}-A\right)\left(B\xi\left(\frac{p}{p_0}\right)^{\gamma-1}+C\right)^{-1}=\varsigma\left(p,\gamma\right) \tag{S.22}$$

where the stress-stiffening exponent γ is the intrinsic property with a value of 1.22.

Finally, the turgor pressure can be expressed as eqn (S.23) by substituting eqn (S.21) and (S.22) into eqn (S.19):

$$\frac{k}{\xi p_0 R}=\frac{a}{\varsigma}\left(\frac{p}{p_0}\right)^{\gamma}\ln\left(\frac{\varsigma}{\xi}\left(\frac{p_0}{p}\right)^{\gamma-1}+b\right)+\frac{c}{\varsigma}\left(\frac{p}{p_0}\right)^{\gamma} \tag{S.23}$$

Since p_0, γ, ξ, a, b and c are all known, the turgor pressure p can be obtained by solving eqn (S.23) with inputting the measured cell radius *R* and stiffness *k* from AFM experiments. Once p is known, the circumferential Young's modulus $E_{\perp}$ can then be extracted by solving eqn (S.19) with inputting the bacterial envelope thickness and stiffness. The axial Young's modulus $E_{\parallel}$ is equal to $0.47E_{\perp}$.

In our study, the extracted turgor pressures for *K. pneumoniae* cells in Milli-Q water and 100 mM $CaCl_2$ solution are 212 ±7 kPa and 59 ±3 kPa, respectively. The extracted orthotropic moduli for the cells in the Milli-Q water are 516 ± 60 MPa in the circumferential direction and 243 ± 28 MPa in the axial direction while those for the cells in $CaCl_2$ solution are 87 ± 17 MPa in the circumferential direction and 40 ± 8 MPa in the axial direction, respectively.

5.2. Verification of the Developed Scaling Rules by Fitting the Experimental Data in Literature

In the work of Deng et al.,[3] they combined their eqn (2), the relationship $E_{\perp}t=E_0t\left(p/p_0\right)^{\gamma}$, and the information obtained by FEM simulation (Fig. 4) to fit their AFM experimental data (Fig. 3). In this method, the lateral stretching modulus[5] λ ($\lambda=E_0t$)and the radius (R_0) of the

bacterium at a reference turgor pressure (p_0), together with the stress-stiffening exponent γ, determine the extracted values of the bacterial turgor pressure and envelope elasticity. In our method, these values are determined by eqn (S.19) and (S.20), and $E_{\perp}t=E_0t\left(p/p_0\right)^{\gamma}$. Under the conditions of $p_0=5\,\text{kPa}$ and $\gamma=1.22$, Deng et al. obtained $\lambda=0.026$ N/m and $R_0=464$ nm by using their method to fit their AFM data, and we obtained $\lambda=0.029$ N/m and $R_0=410$ nm by using our method to fit the same set of data. For the same set of data under the conditions of $p_0=29\,\text{kPa}$ and $\gamma=1.22$, it can be obtained $\lambda=0.22$ N/m and $R_0=550$ nm by using Deng's method, and $\lambda=0.25$ N/m and $R_0=580$ nm by using our method. In both cases, the results are highly consistent with each other. This excellent agreement indicates the good reliability of our developed rules.

6. Stability of the Identified Solutions

FEM simulations allow us to determine the explicit dimensionless functions (eqn (S.19) and (S.20)) with dimensionless parameters $pR/\left(E_{\perp}t\right)$ and $E_{\perp}t/\left(pR_0\right)$ varying in a wide range of values. Determining the turgor pressure and the cell envelope elasticity using eqn (S.19) and (S.20) represents an inverse problem.[13] The reliability of the equations can be assessed by analyzing the stability of the inverse problem. The stability is determined by the sensitivity of the developed rules to small changes in the experimentally measured parameters and can be quantitatively evaluated by the condition number.[10, 13]

The condition number of the turgor pressure can be defined as

$$\psi_1\left(\tilde{p}\right)=\frac{\Pi_3\left(\tilde{p}\right)}{p\,\partial\Pi_3\left(p\right)/\partial p} \tag{S.24}$$

where the dimensionless function $\Pi_3(\tilde{p}) = a\varsigma^{-1}(\tilde{p})^{\gamma}\ln\left(\varsigma\xi^{-1}\tilde{p}^{1-\gamma}+b\right)+c\varsigma^{-1}\tilde{p}^{\gamma}$, $\tilde{p} = p/p_0$.

To determine the condition number of the circumferential Young's modulus $E_{\perp}$, we firstly need to combine eqn (S.21) and (S.22) and the stress stiffening rule $E_{\perp} = E_0(p/p_0)^{\gamma}$ to obtain

$$E_{\perp} = (Rp_0\xi/t)\left(\xi\left(\frac{p_0}{p}\right)-A\left(\frac{p_0}{p}\right)^{\gamma}\right)^{-1}\left(B\xi\left(\frac{p}{p_0}\right)^{\gamma-1}+C\right) = \Gamma(p,R) \tag{S.25}$$

Then the relative error of $E_{\perp}$ can be given as

$$\delta_{E_{\perp}} = \frac{p}{\Gamma}\frac{\partial\Gamma(p,R)}{\partial p}\delta_p + \frac{R}{\Gamma}\frac{\partial\Gamma(p,R)}{\partial R}\delta_R = \psi_2\delta_p + \delta_R \tag{S.26}$$ [14]

where ψ_2, δ_p and δ_R are the condition number of $E_{\perp}$, the relative error of the turgor pressure and the radius of bacterial cells, respectively. $E_{\parallel}$ has the same condition number as $E_{\perp}$ because they are linearly related ($E_{\parallel} = \alpha E_{\perp}$).

The obtained condition numbers (ψ_1 and ψ_2) of the turgor pressure and the orthotropic elastic modulus are 0.90 and 1.21 for the bacterial cells in Milli-Q water, respectively, and 0.91 and 1.21 for the cells in 100 mM $CaCl_2$ solution, respectively. The results indicate that the obtained turgor pressure and envelope elasticity are reliable on the consideration of that the condition numbers in all cases are close to one.[14] In addition, we also computed the condition numbers for a wide range of scaled turgor pressures between 0.03 and 17.2, corresponding to turgor pressures between 1 – 500 kPa. In addition, according to the stress stiffening rule, $E_{\perp}$ are ranged between 0.68 and 1576 MPa when the scaled turgor pressures are in the range between 0.03 and 17.2.

As shown in Fig. S5, the condition numbers are all close to one, indicating that our developed rules are reliable for wide ranges of turgor pressures and elastic moduli.

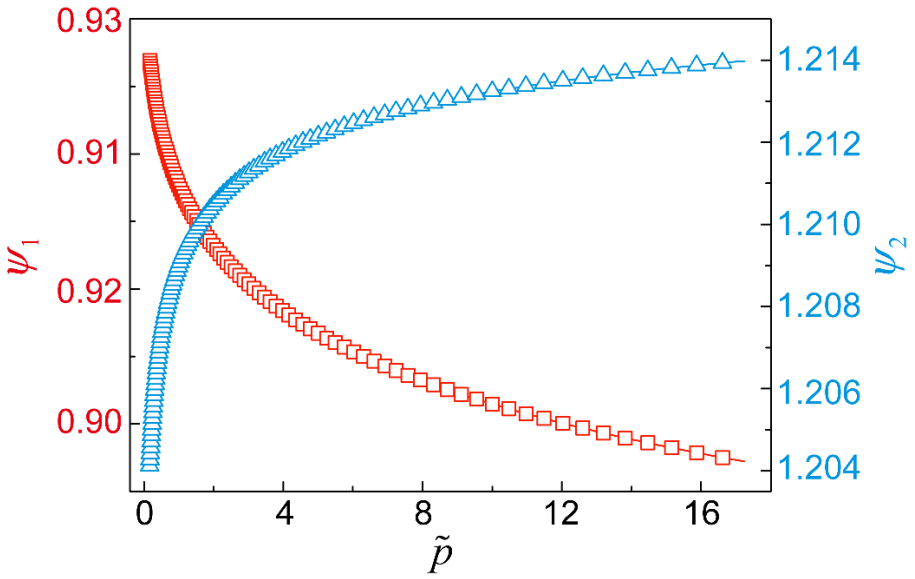

Fig. S5 The condition numbers (ψ_1 and ψ_2) for the turgor pressure and Young's modulus, respectively.

References

1. T. Ohyama, S. Mugikura, M. Nishikawa, K. Igarashi and H. Kobayashi, *J. Bacteriol.*, 1992, **174**, 2922–2928.
2. T. Pilizota and J. W. Shaevitz, *Plos One*, 2012, **7**, e35205.
3. Y. Deng, M. Sun and J. W. Shaevitz, *Phys. Rev. Lett.*, 2011, **107**, 158101.
4. A. Boulbitch, B. Quinn and D. Pink, *Phys. Rev. Lett.*, 2000, **85**, 5246–5249.
5. M. Arnoldi, M. Fritz, E. Bauerlein, M. Radmacher, E. Sackmann and A. Boulbitch, *Phys. Rev. E*, 2000, **62**, 1034–1044.
6. A. E. H. Love, *Proc. R. Soc. London*, 1888, **43**, 352–353.
7. C. Truesdell, *Linear Theories of Elasticity and Thermoelasticity: Linear and Nonlinear Theories of Rods, Plates, and Shells*, Springer, New York, 2013.
8. Y.-T. Cheng and C.-M. Cheng, *Appl. Phys. Lett.*, 1998, **73**, 614–616.
9. M. Dao, N. v. Chollacoop, K. Van Vliet, T. Venkatesh and S. Suresh, *Acta Mater.*, 2001, **49**, 3899–3918.
10. M. G. Zhang, Y. P. Cao, G. Y. Li and X. Q. Feng, *J. Mech. Phys. Solids*, 2014, **68**, 179–196.
11. G. I. Barenblatt and G. I. Barenblatt, *Scaling, self-similarity, and intermediate asymptotics: dimensional analysis and intermediate asymptotics*, Cambridge University Press, Cambridge, 1996.
12. D. P. Holland and A. E. Walsby, *J. Microbiol. Methods*, 2009, **77**, 214–224.
13. M. G. Zhang, Y. P. Cao, G. Y. Li and X. Q. Feng, *Biomech. Model. Mechanobiol.*, 2014, **13**, 1–11.
14. Y. P. Cao and J. Lu, *Acta Mater.*, 2004, **52**, 1143–1153.